VFAST Transactions on Mathematics
http://vfast.org/journals/index.php/VTM@ 2023, ISSN(e): 2309-0022, ISSN(p): 2411-6343
Volume 11, Number 2, July-December, 2023 *pp: 174-197*

Morphological Investigation of Lamellae Patterns in Diblock Copolymers under Change of Thickness and Confinement in Polar Geometry

Muhammad Javed Iqbal[1], **Inayatullah Soomro**[1], **Maryam Bibi**[2], **Rab Nawaz Mallah**[1]

[1]Department of Mathematics, Shah Abdul Latif University, Khairpur, Pakistan;
[2]Department of Mathematics, NCB & E Lahore, Sub Campus Bahawalpur, Pakistan

Keywords:
Computational modelling, Diblock copolymers, Lamellae forming system, Finite difference method.
Subject Classification:
numerical simulation of PDE'S.

Journal Info:
Submitted:
November 5, 2023
Accepted:
December 27, 2023
Published:
December 31, 2023

Abstract Mathematicians work with experimental researchers to predict new morphologies of soft materials that have potential applications in nanotechnology. In this study, a novel lamellar morphology is presented for which a diblock copolymer system confined within a polar geometry is confined and a cell dynamics simulations (CDS) model is applied to the polar mesh to investigate the specific effects of confinement on the self-assembly behaviour. The CDS model is an efficient simulation method in which a stencil with a set of 9 points is considered to discretize the Laplacian operator under the FTCS numerical formulation. The evolving lamella morphology through simulations is presented for different sizes of circular-annular pores with and without confinement. A comparative evaluation of the lamella morphologies obtained by simulation versus experimental study is also presented. Symmetric and asymmetric forms of confinement have also been thoroughly investigated.

***Correspondence Author Email Address:**
mjaved.iqbal@salu.edu.pk
DOI: 10.21015/vtm.v11i2.1675

1 Introduction

The properties of soft materials are between liquids and solids, the discovery of which has revolutionized nanotechnology. These materials include polymers, colloids, liquid crystals, and surfactants. These materials are flexible, sensitive, functional and durable. Mathematicians are engaged in the discovery and prediction of new morphologies of these materials through computational modelling and simulation, enabling the development of nanodevices [11, 12, 19, 24, 46]. Two polymeric blocks joined by chemical bonds form a diblock copolymer system. For the past decade, theoretical scientists have been investigating how polymers self-assemble in the melt state of this system and how their morphologies are affected in the presence and absence of external influences [22, 33]. Diblock copolymers are capable of self-assembling into nanoscale structures with sizes ranging from 10 to 100 nm. Because of this feature, block copolymers show promise for applications requiring molecularly ordered structures at the nanoscale scale [16, 42]. The chemical incompatibility of the polymer blocks in block copolymers causes them to separate. This allows them to spontaneously produce a wide variety of nanostructured patterns, tuned by parameters like composition ratio, block design, block strength, molecular properties, and external confinement geometries. These parameters lead to the formation of a large variety of controllable, self-assembled shapes [7, 15, 27, 36, 45].

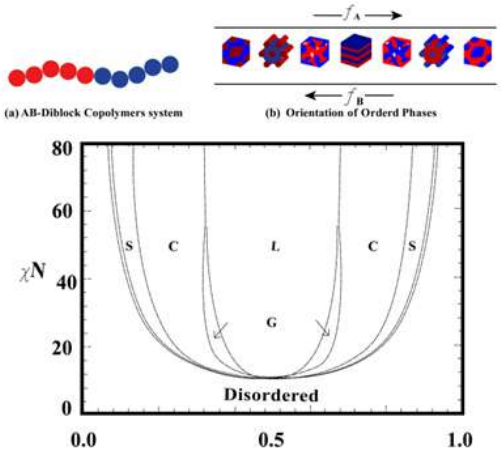

Figure 1. Bulk phase diagram of diblock copolymers system

The bulk phase diagram of diblock copolymers (Figure 1) has been well studied theoretically and practically, revealing a variety of microdomain structures capable of self-assembly in the melt state. Depending on the length of the respective block and the temperature used, structures such as lamellae, cylinders, gyroids, and other shapes have been found. Diblock copolymer systems enable the creation of a wide range of nanostructured patterns [2, 3, 5, 9, 13, 14, 40].

The term "confinement" describes the process of constraining the geometry of a system through physical barriers such as films, substrates, and nanopores. This presents the interface at which the internal phase separation behaviour of the microdomains competes against their growth by lowering their energy. Thin film pores are common examples of confinement, which can cause long-range ordering. Domains rearrange to form patterns that satisfy boundaries. Often, the lamellae are aligned parallel to the interface. The shape is guided by confinement length scales such as circles in small pores, cylinders in medium pores,

and lamellae when larger than the natural spacing. Discouraging boundary forms can lead to the formation of increasingly complex self-contained patterns. Both computational models and experiments shed light on how confinement affects phase behaviour, orientation, and defects. Technologically, controlling self-assembly through confinement is advantageous for applications in drug administration, membranes, and nanopatterning. When polymer blocks are stacked in a periodic pattern, the alternating layers of each block produce a large number of lamellae. The block size ratio is one of the factors that determines the width of layers. Lamellae are forced to rearrange when they are confined between surfaces that are closer to each other than the equilibrium lamellar spacing.[1, 8, 21, 38].

Lamellar layers can align themselves in a vertical, perpendicular or mixed manner concerning the substrate using thin film geometries. Some artefacts may occur, such as periodic holes or parallel lines. Confinement introduces competing effects of minimizing surface-lamella and lamella-lamella domain interface energies. This leads to unique self-assembled structures not seen in the bulk. Both experimental techniques such as atomic force microscopy and computational modeling have been used to study lamellae recovery under nanoscale confinement. Understanding these effects provides a way to control block copolymer self-assembly and direct the composition of nanostructured materials with applications in nanolithography, biomaterials, and more. Lamellae are a frequently ordered structure seen in diblock copolymer melts, where sheets of each block alternate and pack in a layered pattern. To reduce interactions at the interface, the lamellae of these systems adopt distinct orientations when enclosed within nanoscale geometries. Gaining insight into the creation of nanostructured lamellae under confinement opens up possibilities for manipulating material properties via self-assembly [4, 28, 31, 39, 41].

Boundaries can be naturally accounted for in the formulation by transforming the physical issue into a boundary-fitted coordinate system such as polar, spherical, or cylindrical coordinates. By doing this, utilizing standard Cartesian grids to handle interfaces with irregular shapes eliminates problems that would otherwise develop. The modified coordinates align with the boundary geometry, streamlining the depiction and facilitating precise confinement effect simulation irrespective of boundary intricacy. Block copolymer self-assembly patterns are directed by confinement within cylindrical pores, and this may be accurately modelled numerically thanks to the use of a polar coordinate system, which incorporates the boundary geometry into the problem definition. Because of problems with the boundary geometry, modelling block copolymer self-assembly under curvilinear confinement is difficult when using cartesian coordinates. The problem is transformed by using polar coordinates, which leads to the implicit and natural definition of the cylindrical boundary as $r = R$. This makes it possible to discretize and rewrite the governing equations on a uniform polar grid that follows the boundary. This polar coordinate representation offers an accurate means of simulating how cylinder confinement dictates patterns of self-assembly while avoiding problems seen when using a cartesian grid [17, 23, 34, 35, 37].

Depending on temperature and material, compatible diblock copolymer melts containing equal parts of two incompatible polymer blocks can exhibit ordered or disordered microphase separation states. Entropy takes over at high temperatures, causing the blocks to randomly mix and create a chaotic state. To reduce the repulsive interactions between the blocks, as the temperature drops, the energy facilitates the microphase separation into ordered structures such as spheres, cylinders, or lamellae. A disorder transition occurs between these states in an orderly manner depending on the relative contribution of enthalpic and entropic forces. The formation of microphase separation structures in asymmetric diblock copolymers, characterized by uneven volumes of the two polymeric blocks, is highly dependent on the minority block's relative volume fraction. The morphology changes from cylinders to a complicated bi-

continuous gyroid network and finally to a layered lamellar structure with increasing minority lamellae thickness as the minority proportion rises. More intricate structures, such as perforated layers, can also arise for intermediate asymmetries between the spherical and cylindrical morphologies, contingent on variables such as overall chain length and segregation strength [25, 29].

Controlling pore geometries and characterizing nanostructures are difficult tasks for experimental research on diblock copolymer formation under confinement. To systematically analyze lamellar morphologies as a function of polar confinement parameters, which are challenging to explore experimentally, cell dynamic simulation offers a potent complementary method. Creating a thorough phase diagram and clarifying the mechanisms regulating self-assembly under idealized pore conditions are the goals of this computational work, which will also provide basic insights into spinodal breakdown routes and serve as a guide for future experimental design. Thin films of block copolymer may find use in biomaterials, energy harvesting, optics, electronics, sensors and nanolithography. Due to competing surface and curvature energy, unique self-assembly phenomena arise when diblock copolymer lamellae are restricted in polar geometries like cylindrical pores. This work aims to clarify how morphological alterations caused by polar confinement differ from those caused by bulk lamellae. Comprehending these impacts will enable the regulation of feature dimensions and alignment for technological uses necessitating extended ordering of nanoscale domains. Given this research gap, we present our research and study of confinement effects in polar geometries to predict novel morphologies in symmetric $f_A = f_B$ and asymmetric $f_A \neq f_B$ diblock copolymers.

2 Methodology

2.1 Discretization

Continuous physical domains must be discretized into a uniform computing grid or space to apply finite difference approaches for numerically solving partial differential equations. Nevertheless, this discretization is not compatible with cartesian coordinate systems for domains whose boundaries are irregular. These problems are solved by curvilinear coordinate systems, like polar grids (Figure 2), which enable the computational grid to adapt to the borders of physical domains like pores or particles without experiencing significant clustering or cut cells. Dispersing points when gradients are minor, improves computational efficiency and allows for the precise resolution of big gradients close to boundaries through point clustering. Curvilinear coordinates, thus, are well-suited for simulations of issues involving domains with curved boundaries, such as confinement, since they preserve grid uniformity while meeting the essential requirements of finite difference methods for accuracy in resolving large gradients and efficiency [20].

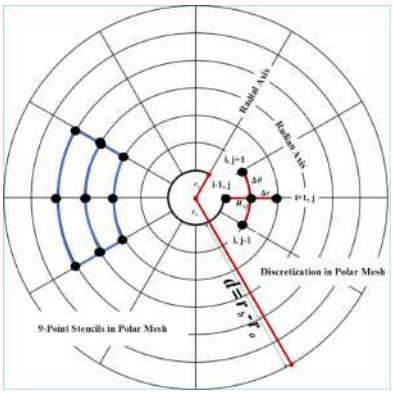

Figure 2. Discretization in polar mesh and 9-point stencils

The point $u_(i,j)$ is an averaging point of the other eight neighbouring and mixed neighbouring points. Δr is interval of radial follows periodic boundary conditions and $\triangle\theta$ is radian interval in any cell follows the reflective boundary conditions. Pore size d is the difference between the external radius r_b and internal radius r_a.

2.2 Cell dynamic simulation

The macromolecule of diblock copolymers (Figure 3) is discretized into a 9-point stencil in polar mesh for isotropic Laplacian involved in the CDS model. FORTRAN codes are generated to run simulations to predict novel Lamellae morphologies for both symmetric and asymmetric study of diblock copolymers systems. In the end, predicted morphologies are provided in comparison with existing experimental morphologies to validate our proposed study.

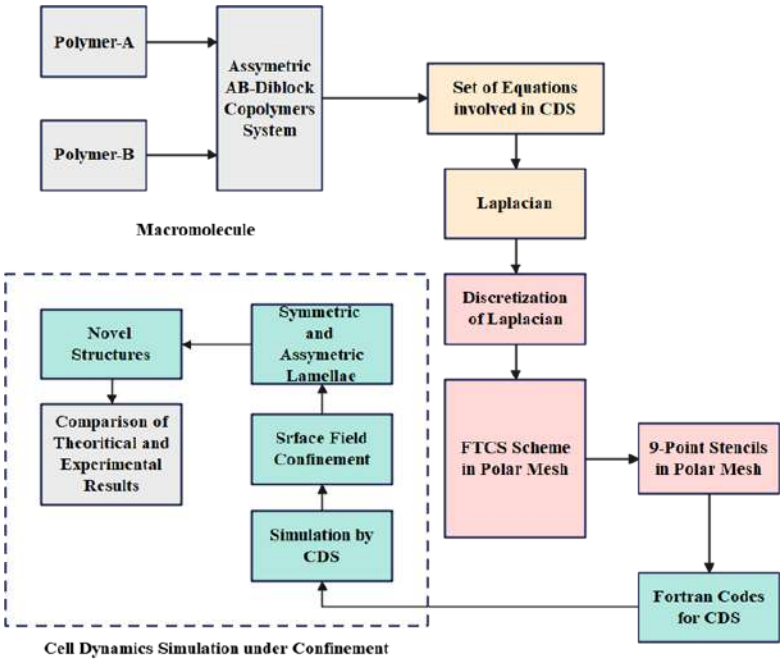

Figure 3. Algorithm of cell dynamic simulations model

The order parameter $\psi(t, i)$ of the diblock copolymers system.

$$\psi = \phi_A - \phi_B + (1 - 2f). \tag{1}$$

where $f = \frac{N_A}{N_A+N_B}$ The rate of change in ψ is given as

$$\frac{\partial\psi(r,t)}{\partial t} = -\nabla j(r,t) \tag{2}$$

$j(r, t)$ is flux, given as The rate of change in ψ is given as

$$j(r,t) = -M\nabla\mu(r,t) \tag{3}$$

where $\mu(r, t)$ is given as

$$\mu(r,t) = \frac{\delta F[\psi]}{\delta\psi} \tag{4}$$

The rate of change in ψ associated with CHC is

$$\frac{\partial\psi}{\partial t} = M\nabla^2\left(\frac{\delta F[\psi]}{\delta\psi}\right) + \eta\xi(r,t). \tag{5}$$

Here $M = 1$ and η is the amplitude of noise and $\xi(r, t)$ is a gaussian noise follows $(0, 1)$. The Product KT of Boltzmann constant K and absolute Temporal constant T is connected with scale of microscopic thermal energy. We divide the free energy Functional by KT and get.

$$F[\psi(r)] = \int dr\left[H(\psi) + \frac{D}{2}\left|\nabla\psi\right|^2\right] + \left(\frac{B}{2}\right)\int dr' G(r - r')\psi(r)\psi(r'). \tag{6}$$

The free energy is calculated with $H[\psi]$

$$H[\psi] = (-\frac{\tau}{2}) + (\frac{A}{2})(1-2f)^2\psi^2 + v(1-2f)\psi^3 + (\frac{u}{4})\psi^4 \tag{7}$$

Here τ is a temporal parameter, and A, v and u All of these parameters are related to the properties of the molecule and are all remarkably stable phenomenological constants. Here

$$\tau = A(1-2f)^2 - \tau'$$

and

$$\tau' = -(N\chi - \frac{s(f)}{4f^2(1-f)^2})$$

$$D = \frac{b^2}{48f}(\frac{1}{1-f})$$

$$B = (\frac{3}{2Nbf(1-f)})^2$$

Here χ is the parameter used to interactive parameter between the blocks A and B, N is the degree of polymerization, b is the segment length of blocks chain. Now, our CDS model equation is given as

$$\frac{\partial\psi}{\partial t} + \nabla.(\upsilon\psi) = \eta\xi(r,t) + M\nabla^2\frac{\delta F[\psi]}{\delta\psi} \tag{8}$$

Numerically, we the CDS equation is given as [10, 26]

$$\begin{aligned}\psi(\mathbf{n},t+1) &= \psi(\mathbf{n},t) - \{\langle\langle\Gamma(\mathbf{n},t)\rangle\rangle\Gamma(\mathbf{n},t) + B\psi(\mathbf{n},t) - \eta\xi(\mathbf{n},t) \\ &\quad + \frac{1}{2}\tilde{\gamma}\tilde{y}[\psi(n_x,n_y,n_z+1,t) - \psi(n_x,n_y,n_z-1,t)]\}\end{aligned} \tag{9}$$

In this equation $\langle\langle\Gamma(\mathbf{n},t)\rangle\rangle\Gamma(\mathbf{n},t)$ is 9-point isotropic stencils of Laplacian. Here

$$\Gamma(\mathbf{n},t) = g(\psi(\mathbf{n},t) - \psi(\mathbf{n},t+1) + D\{\langle\langle\psi(\mathbf{n},t)\rangle\rangle\psi(\mathbf{n},t)\} \tag{10}$$

In this equation $\langle\langle\Gamma(\mathbf{n},t)\rangle\rangle\Gamma(\mathbf{n},t)$ is 9-point isotropic stencils of Laplacian.

$$g(\psi) = \psi[1 - A(1-2f)^2 + \tau] + \psi^2(1-2f)\upsilon - \psi^3 u \tag{11}$$

The 9-point isotropic approximation of discrete Laplacian is derived in the polar geometry and given as

$$\begin{aligned}\langle\langle\Gamma(\mathbf{n},t)\rangle\rangle &= \alpha\sum_{i=1}^{n_r}\sum_{j=1}^{n_\theta}\left[\frac{1}{3(\triangle r)^2}X + \frac{1}{6(r\Delta r)}Y + \frac{1}{3(r\Delta\theta)^2}Z\}\right] \\ &\quad - \sum_{i=1}^{n_r}\sum_{j=1}^{n_\theta}\psi_{i,j}\end{aligned} \tag{12}$$

Here

$X = \{\psi_{i+1,j+1} - 2\psi_{i,j+1} + \psi_{i-1,j+1} + \psi_{i+1,j} + \psi_{i-1,j} + \psi_{i+1,j-1} - 2\psi_{i,j-1} + \psi_{i-1,j-1}\}$,

$Y = \{\psi_{i+1,j} - \psi_{i-1,j} + \psi_{i+1,j+1} - \psi_{i-1,j+1} + \psi_{i+1,j-1} - \psi_{i-1,j-1}\}$,

$Z = \{\psi_{i,j+1} + \psi_{i,j-1} + \psi_{i-1,j+1} - 2\psi_{i-1,j} + \psi_{i-1,j-1} + \psi_{i+1,j+1} - 2\psi_{i+1,j} + \psi_{i+1,j-1}\}$ and waiting factor

$\alpha = \left[\frac{3(r\Delta r\Delta\theta)^2}{2\{(r\Delta\theta)^2+(\Delta r)^2\}}\right]$

3 Simulations and Results

3.1 Lamellae forming system

Computational and mathematical simulations are used to study the intrinsic phase separation behavior of the confined diblock copolymer system and to account for the preferential affinity of one kind of polymer block towards the confining pore surface. This is accomplished inside the simulation methodology by designating an energy bias for one block at the pore-polymer interface. Then, in addition to confinement size and geometry, the effects of this additional competing element of surface energetics are investigated to offer mechanistic insights into how surface-directed self-assembly affects the morphological structures beyond those merely driven by bulk segregation inclinations. We have studied the diblock copolymers system in two dimensions and predicted the novel Lamellae morphologies confined in circular annular pores for their different pore sizes. The cell dynamic simulations are carried out by using periodic boundary conditions in the angular domain $0 \leq \theta \leq 360$ with angular step $\theta = \frac{2\pi}{360}$ and reflected boundary conditions in radial domain r with radial step $\Delta r = 0.1$. Pore d is the circular region between two concentric circles with fixed interior radius $r_a = 3, 5, 7$ while variation in outer radius defines the variation in pore sizes. The affinity of one block of the system with walls is described by the interactive strength α. The neutral wall study is investigated by taking $\alpha = 0$ and for the attractive walls study we set $\alpha = 0.2$. The simulation is done for 1 million time steps.

Table 1 shows the parameters used CDS model to investigate the lamella-forming system in the absence

Table 1. *CDS parameters for development of Lamellae forming system*

A	B	D	u	v	f	τ	Δr	Δt	α	$\Delta\theta$
1.50	0.20	0.50	0.50	2.30	0.50	0..36	0120	0.10	0.00	0.017453292

of attractive walls. Both blocks in the system are set $f_A = 0.5 = f_B$ to study the Lamellae morphologies in symmetric blocks.

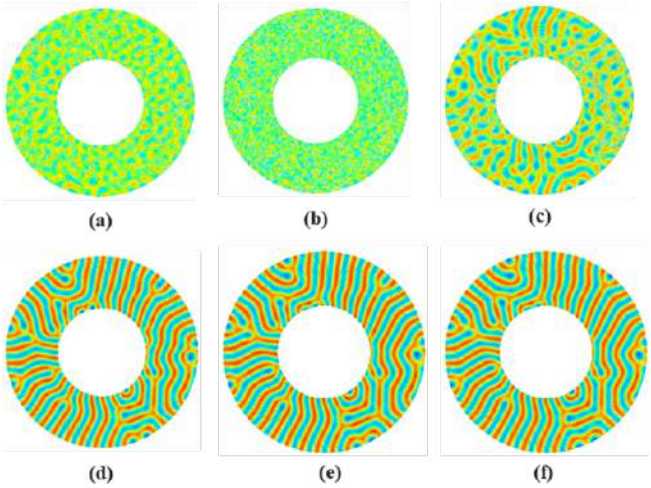

Figure 4. Lamellae forming system with neutral walls

In Figure 4, we have presented the systematics formulation of Lamellae in a symmetric diblock copolymers system in various time steps. For this purpose, we have fixed the internal radius r_a = 5 and set the external radius r_b = 11 to get pore size d = 6. We have recorded the formulation of morphologies at different time steps t=10 (Figure 4a), t=100 (Figure 4b), t=1000 (Figure 4c), t=10000 (Figure 4d), t=100000 (Figure 4e), and t=1000000 (Figure 4f) respectively. Before the blocks start to separate from one another in the early stages of the simulation, they are mixed haphazardly and without any kind of structure. Gradually, when strongly interacting blocks segregate, loosely defined domains appear randomly. In due course, the blocks completely split into parallel, well-defined lamellar layers that are consistently spaced and reflect the equilibrium morphology as long-range order develops.

3.2 Symmetric Lamellae forming system with neutral walls

In Figure 5, We have presented the lamellae formations between two concentric circles for polar geometries without attractive walls. We have fixed the internal circle with a radius r_a = 3 and the external circle with radius r_b = 6, 7, 8, 11, 12, 13 to observe the variation in pore sizes from d = 3, 4, 5, 8, 9 and 10 respectively. Simulation is carried out for one-million-time steps. The interactive strength of attractive walls is set at α = 0.

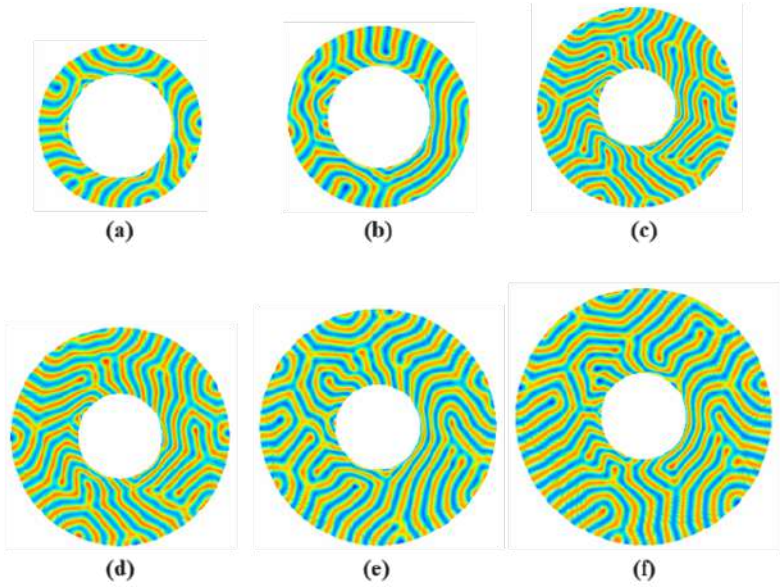

Figure 5. Symmetric Lamellae forming system r_a = 3 with neutral walls for various pore sizes d=3 in (a), d=4 in (b), d=5 in (c), d=8 in (d), d=9 in (e) and d=10 in (f).

The simulation investigated how enlarging a circular pore affects the morphological structures that a restricted block copolymer system forms inside of it. A radially directed parallel array of u-shaped strips was seen at the smallest pore size of 3 units. The initially homogeneous parallel strips, however, started to warp and change into various orientations, such as alternating *U*-shaped and perpendicular *Y*-shaped geometries, as the pore size increased. Even greater pore sizes produced highly curved winding cylinders and intricately structured slanted w-shaped strips as the relaxation of confinement made it possible to minimize interfacial energy through a variety of orientations and continuous polar shapes. Interestingly, a perforated or hole-containing morphology did not materialize even at the largest pore sizes, indicating

that this specific block copolymer, when spatially restricted within a circular pore, preferentially adopts non-perforated morphologies over other possible microdomain types.

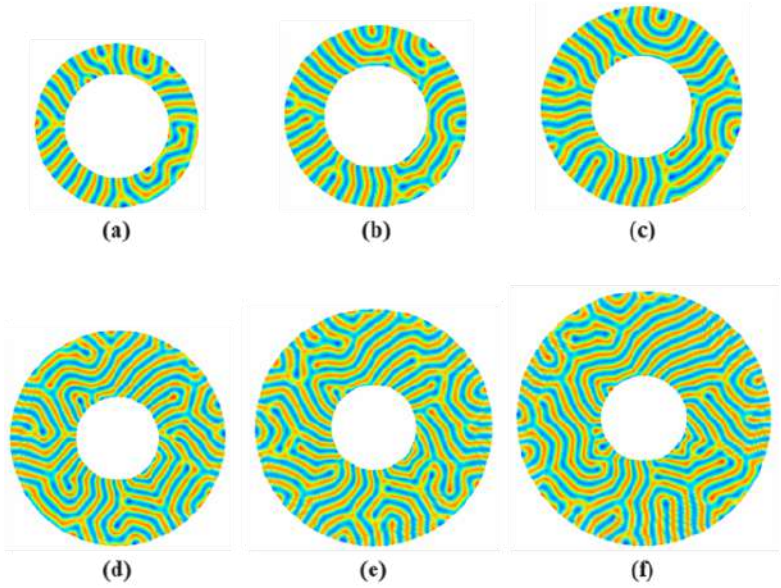

Figure 6. Symmetric Lamellae forming system at r_a = 5 with neutral walls for various pore sizes d=3 in (a), d=4 in (b), d=5 in (c), d=8 in (d), d=9 in (e) and d=10 in (f).

The lamellae formations limited in concentric rings for polar geometries without attractive walls are shown in Figure 6. To observe the fluctuation in pore sizes from $d = 3, 4, 5, 8, 9$, and 10, respectively, we have fixed internal circles with radius $r_a = 5$ and external circles with radius $r_b = 8, 9, 10, 13, 14$ and 15. The simulation runs for a million iterations. At $\alpha = 0$, the walls' interaction strength is fixed. The simulation that looked at how a circular pore's internal radius affected the morphology of block copolymers revealed that, at small internal radii, expanding the unconstrained inner cavity led to the formation of u- and y-shaped striped structures that were oriented both parallel and perpendicular to the radial direction. This phenomenon was similar to increasing the overall pore size. Enlarging the inner surface, however, preferentially stabilized well-defined, uniformly parallel alignments of lamellar-like layers along the circumferential edge rather than more intricate non-parallel orientations or transformations into various shapes, in contrast to altering the pore size. This suggests that rather than further disrupting morphologies, as was observed when the total pore size was increased instead of just the internal radius, expanding the inner pore surface primarily served to relieve geometric frustrations driving normal orientations while maintaining a degree of overall confinement. This resulted in a clearer parallel alignment of strips parallel to the circular boundary. Figure 7 displays the lamellae formations between two concentric circles for polar geometries without attractive walls that are visually pleasing. We have fixed internal circles with a radius $r_a = 7$ and external circles with a radius $r_b = 10, 11, 12, 15, 16$ and 17 to study the variation in pore diameters from $d = 3, 4, 5, 8, 9$, and 10, respectively. One million iterations of the simulation are performed. The interaction strength between the walls is fixed at $\alpha = 0$.

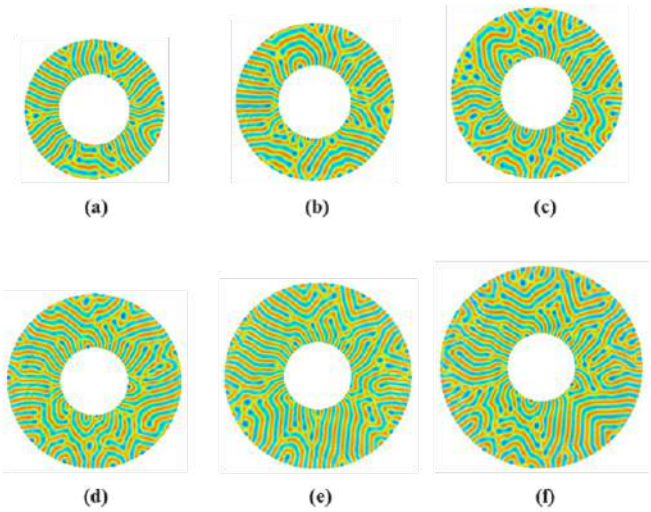

Figure 7. Symmetric Lamellae forming system at r_a = 7 with neutral walls for various pore sizes d=3 in (a), d=4 in (b), d=5 in (c), d=8 in (d), d=9 in (e) and d=10 in (f).

The simulation demonstrated that when the internal radius of the circular pore was raised from 5 to 7 units, the lamellar morphology created a more complex mixed orientation with both parallel and perpendicular domains. Specifically, perforated hole formations began to emerge within the structure, and the lamellar strips, which were primarily parallel or normal, displayed a greater range of tilted and curved orientations at lower internal radii. It's interesting to note how randomly parallel strip sets with perpendicular orientations coexisted. This indicated that the geometric tensions that previously exclusively motivated normal or parallel layouts have loosened. In contrast to higher degrees of orientational order stabilized at smaller internal pore cavities, distinct orientational domains coexisted and displayed partial relaxation of confinement effects when slanted, curved, and parallel-perpendicular strips were mixed. Overall, the mixed morphology revealed a less limited intermediate state as compared to previous studies.

3.3 Symmetric Lamellae forming system with attractive walls

A diblock copolymer that forms symmetric lamellae and is confined between walls that preferentially attract one of the polymer blocks is modelled using computational simulations. The lamellar morphology orients itself normally to the surfaces at low attraction strengths between the walls and one block. This minimizes the interfacial area between domains of alternating blocks and satisfies the surfaces' preferential wetting. However, the influence of the surfaces becomes dominant above a critical strength of attraction, frustrating the equilibrium lamellar structure and reorienting the domains parallel to the confining interfaces.

Table 2. *CDS parameters for development of Lamellae forming system*

A	B	D	u	v	f	τ	Δr	Δt	α	$\Delta\theta$
1.50	0.20	0.50	0.50	2.30	0.50	0..36	0120	0.10	0.20	0.017453292

The parameters involved in the CDS model for the simulation of symmetric Lamellae forming (f_A = 0.5 =

f_B) confined in circular annular pores are presented in Table 2. We have set the interactive parameter α = 0.2.

In Figure 8, We have presented the symmetric lamellae formations confined in circular annular pores after discretization of Laplacian in polar geometries. We have fixed the internal circle with radius r_a = 3 and the external circle with radius r_b = 6, 7, 8, 11, 12 and 13 to observe the variation in pore sizes from d = 3, 4, 5, 8, 9 and 10 respectively. Simulations are carried out for one-million-time steps. The interactive strength of attractive walls is set at α = 0.2.

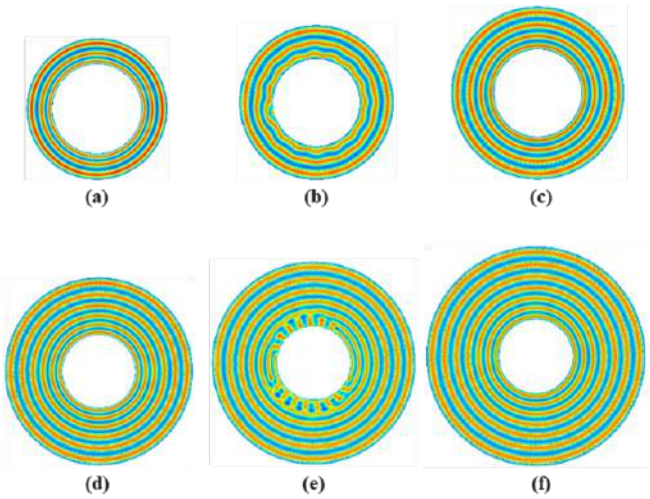

Figure 8. Symmetric Lamellae forming system at r_a = 3 with attractive walls for various pore sizes d=3 in (a), d=4 in (b), d=5 in (c), d=8 in (d), d=9 in (e) and d=10 in (f).

The simulation demonstrated that the lamellar morphology self-organized into concentric rings of lamellar domains within the pore when confinement was applied to the block copolymer system through limitations within a circular pore shape. The creation of concentric layers in line with the circular contours minimizes the curvature stresses imposed by the circular pore borders and their inherent polar symmetry, which is responsible for the orientation of concentric lamellae. More well-formed concentric lamellar structures were able to form and occupy the growing void volume while preserving the curvature-directed alignment around the pore edges when the size of the enclosing pore space was increased proportionately. Enlarging the pore size allowed for a corresponding increase in the number of such concentric lamellar domains filling the expanding confined volume. As a result, it was demonstrated that confinement within the circular boundaries caused lamellae to preferentially align themselves into concentric circles. We have observed some elongated perforated holes in disordered form at pore size 9.

In Figure 9, We have presented the symmetric lamellae formations confined in circular annular pores after discretization of Laplacian in polar geometries. We have a fixed internal circle with radius r_a = 5 and external circle with radius r_b = 8, 9, 10, 3, 14 and 15 to observe the variation in pore sizes from d = 3, 4, 5, 8, 9 and 10 respectively. Simulation is carried out for one-million-time steps. The interactive strength of attractive walls is set at α = 0.2.The morphology of concentric circular lamellar stacks did not change significantly when the internal pore radius was increased from 3 to 5 units in the simulation. This suggests that the curvature-directed self-assembly that oriented the lamellae into rings aligned with the circular boundaries was not significantly perturbed. However, some localized distortions in the lamellar domains

amid the concentric circles first appeared at a pore size of 6 units.

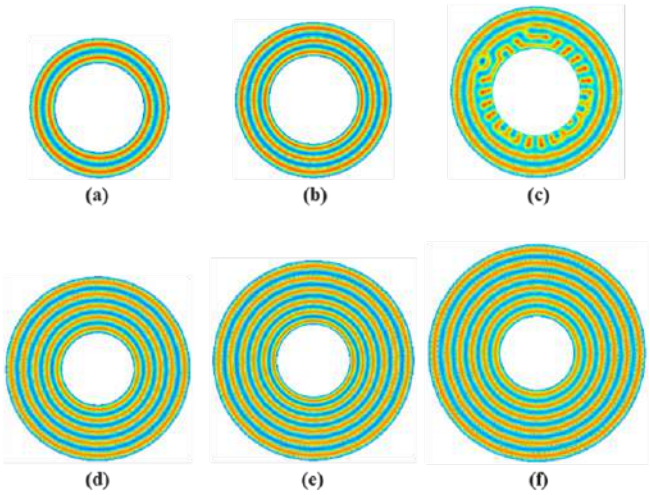

Figure 9. Symmetric Lamellae forming system at r_a = 5 with attractive walls for various pore sizes d=3 in (a), d=4 in (b), d=5 in (c), d=8 in (d), d=9 in (e) and d=10 in (f).

A size-dependent transition where confinement is gradually relaxed to introduce small perturbations to the oriented structure without transforming it entirely is demonstrated by the appearance of distorted lamellae only above a threshold radius of about 6 units, but not at other pore sizes. As a result, expanding the internal cavity within a specific size range did not change the curvature effects' overall concentric organization; however, expanding the cavity beyond a certain point resulted in the introduction of localized instability due to warped lamellar formations among the otherwise well-oriented concentric stacks.

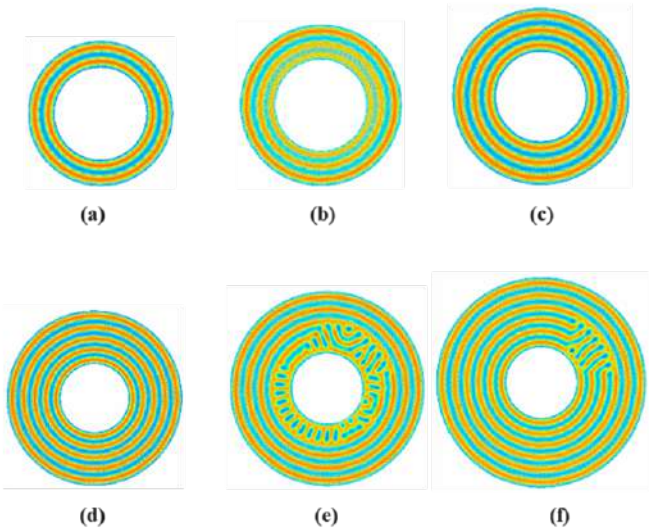

Figure 10. Symmetric Lamellae forming system at r_a = 7 with attractive walls for various pore sizes d=3 in (a), d=4 in (b), d=5 in (c), d=8 in (d), d=9 in (e) and d=10 in (f).

In Figure 10, We have presented the symmetric lamellae formations confined in circular annular pores

after discretization of Laplacian in polar geometries. We have fixed internal circle with a radius r_a = 7 and an external circle with a radius r_b = 10, 11, 1215, 16 and 17 to observe the variation in pore sizes from d = 3, 4, 5, 8, 9 and 10 respectively. Simulation is carried out for one-million-time steps. The interactive strength of attractive walls is set at α = 0.2.

3.4 Asymmetric Lamellae forming system with neutral walls

An asymmetric diblock copolymer with uneven volume fractions of the two blocks which leads to a preferential enrichment of one block at interfaces and a lamellar microphase separation morphology is studied using computational simulations. To minimize the overall interfacial energy between the surface and the favoured block at the interface, the asymmetric composition of this system, which is contained by neutral, non-preferential walls, naturally orients the lamellar domains parallel to the confining interfaces. The simulations shed light on how variables such as volume fraction asymmetry and system size affect the layering periodicity and orientation as they evolve from disordered beginning states. Additionally, they describe the defect structures that appear at domain boundaries. These neutral surface simulations' outcomes provide a crucial starting point for comprehending how asymmetric diblock thin films self-assemble.

The Asymmetric lamellae morphologies are shown in Figure 11 for polar geometries without attractive walls, contained within two concentric circles. For the Asymmetric study of the diblock copolymers system, we have set the volume fraction of both blocks as f_a = 0.48 and f_b = 0.52. To see the variation in pore sizes d = 3, 4, 5, 8, 9 and 10, respectively, we have fixed internal circles with radius r_a = 3 and external circles with radius r_b = 6, 7, 8, 11, 12 and 13. One million iterations of the simulation are performed. Set at α = 0, attractive walls have an interaction strength.The simulation showed that smaller initial pore sizes showed some perforated hole forms and parallel-oriented lamellar strips along the pore boundaries within the neutrally confined, asymmetric system without appealing walls.

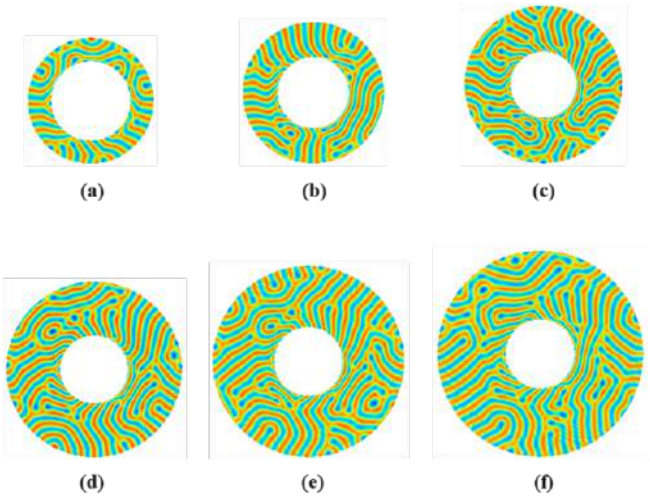

Figure 11. Asymmetric Lamellae forming system at r_a = 3 with neutral walls for various pore sizes d=3 in (a), d=4 in (b), d=5 in (c), d=8 in (d), d=9 in (e) and d=10 in (f).

However, increasing the pore size resulted in the development of sets of perpendicular-oriented lamellar strips scattered among the pore-aligned domains, as well as more perforated holes emerging within the morphology due to further relaxation of constraints against non-uniform structures. In addition, the

expanded area permitted a variety of striped domain forms, such as *u*, λ, and *y*-shaped arrangements, since the bigger pores relieved geometric tensions and permitted different morphologies and orientations other than parallel alignments to reduce interfacial energy. As a result, the self-assembled block copolymer microdomains orientation and morphologies became more heterogeneous and asymmetric as a result of the neutral confinement combined with gradually larger pore diameters.

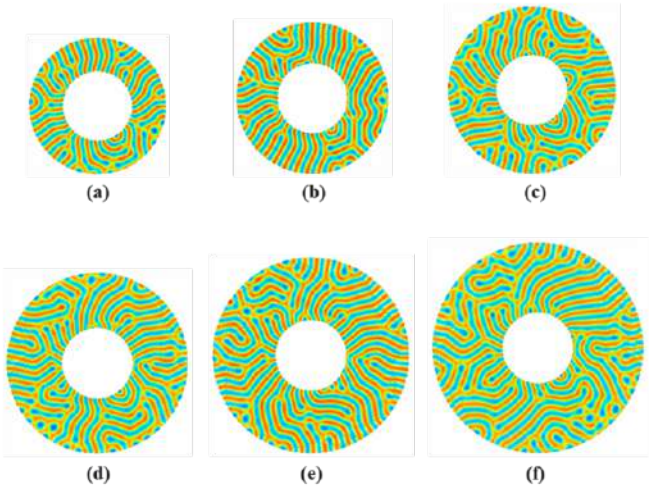

Figure 12. Asymmetric Lamellae forming system at r_a = 5 with neutral walls for various pore sizes d=3 in (a), d=4 in (b), d=5 in (c), d=8 in (d), d=9 in (e) and d=10 in (f).

Figure 12 displays the asymmetric lamellae morphologies for polar geometries with neutral walls enclosed in two concentric circles. The volume fractions of both f_a = 0.48 and f_b = 0.52, have been set for the asymmetric research of the diblock copolymers system. We have fixed internal circles with radius r_a = 5 and external circles with radius r_b = 8, 9, 10, 13, 14 and 15 in order to see the variation in pore sizes from d = 3, 4, 5, 8, 9 and 10, respectively. There are a million simulation runs conducted. Attractive walls have an interaction strength that is set at α = 0. Upon increasing the pore's internal radius, a more intricate mixed morphology emerged within the area, suggesting a greater relaxation of geometric restrictions as compared to just increasing the pore's overall size.

In addition to showing additional stress relief that allowed for non-uniform structures to emerge among the self-assembled block copolymer domains, newly formed perforated hole formations also showed evidence of deformation from their previous shapes at smaller internal radii. The increased unconfinement caused a significant topological remodelling and rearrangement of the microphase separation morphology, as evidenced by the simultaneous development of new holes and distortion of existing ones. These results, along with the previously noted diversity of orientations, highlighted the strong role that localized confinement plays in determining structural development. Specifically, a larger degree of relaxation caused by enlarging the internal pore cavity led to significant disruption and reorganization instead of small-scale morphological changes.

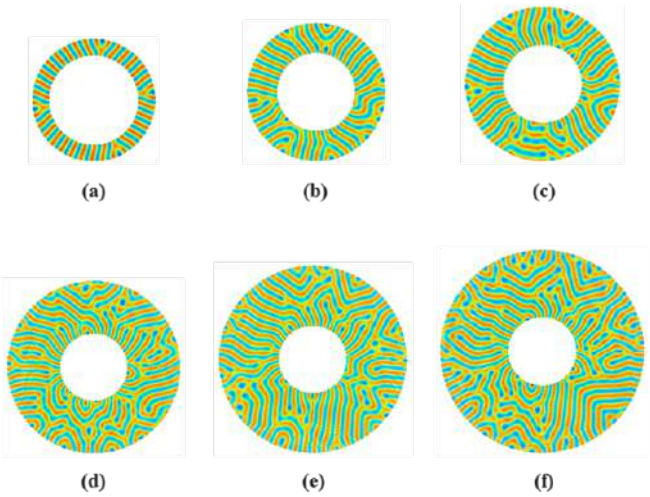

Figure 13. Asymmetric Lamellae forming system at r_a = 7 with neutral walls for various pore sizes d=3 in (a), d=4 in (b), d=5 in (c), d=8 in (d), d=9 in (e) and d=10 in (f)

Figure 13 displays the asymmetric lamellae morphologies for polar geometries with two concentric circles and no attractive walls. The volume fractions of both blocks f_a = 0.48 and f_b = 0.52, have been set for the asymmetric research of the diblock copolymers system. We have fixed internal circles with radius r_a = 7 and external circles with radius r_b = 10, 11, 12, 15, 16 and 17 in order to see the variation in pore sizes from d = 3, 4, 5, 8, 9 and 10, respectively. There are a million simulation runs conducted. Attractive walls have an interaction strength that is set at α = 0. Initially, additional parallel and slanted parallel lamellar strips emerged, projecting along the margins of the pores within this restricted size range, when the internal radius of the circular pore was increased from 5 to 7 units. This demonstrated that the enlarged but relatively small interior volume favourably facilitated the energetically advantageous development and alignment of extra strips running parallel to the circular walls. But instead of being primarily parallel, the morphology evolved into a mixed orientation with a variety of non-uniform nanostructures when the internal radius was increased to considerably larger values than 7 units. Consequently, a transition took place whereby small increases up to seven units preserved partially confined geometries that continued to guide parallel self-organization, but large expansions sufficiently loosened constraints to bring about topological alterations and the heterogeneous assembly patterns typical of a complex mixed morphology.

3.5 Asymmetric Lamellae forming system with attractive walls

Figure 14 displays the asymmetric lamellae morphologies for polar geometries with appealing walls that are encapsulated in two concentric circles. The volume fractions of both blocks, f_a = 0.48 and f_b = 0.52, have been set for the asymmetric research of the diblock copolymers system. We have fixed internal circles with radius r_a = 3 and external circles with radius r_b = 6, 7, 8, 11, 12 and 13 to show the variation in pore sizes from d = 3, 4, 5, 8, 9 and 10, respectively. There are a million simulation runs conducted. Attractive walls have an interaction strength, set at α = 0.2.

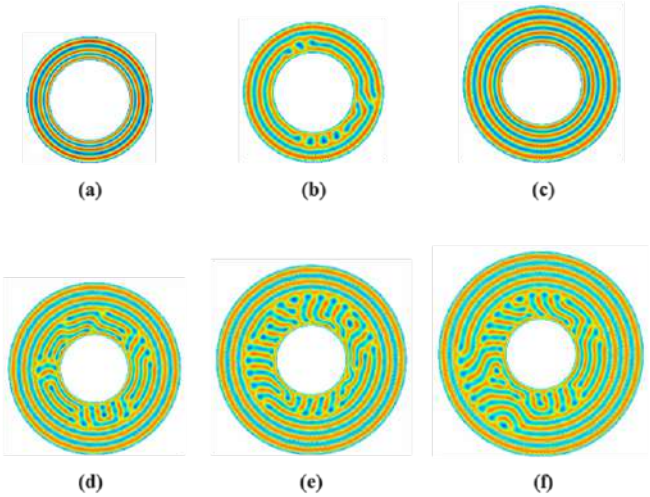

Figure 14. Asymmetric Lamellae forming system at r_a = 3 with attractive walls for various pore sizes d=3 in (a), d=4 in (b), d=5 in (c), d=8 in (d), d=9 in (e) and d=10 in (f).

Due to the strong curvature effects around the polar boundaries, which imposed preferential orientation, concentric circular lamellar structures developed at the smallest internal pore size of 3 in this study of an asymmetric diblock copolymer system under cylindrical confinement within circular pores. Up to a pore size of five, this curvature-driven concentric ordering remained stable. Nonetheless, at increased pore diameters of 8, 9, and 10, the lessened confinement permitted the formation of lamellar strips that were oriented perpendicularly and parallel to the pore walls, as well as the partial development of concentric layers. This release of geometric constraints resulted in the induction of variable domain alignments.

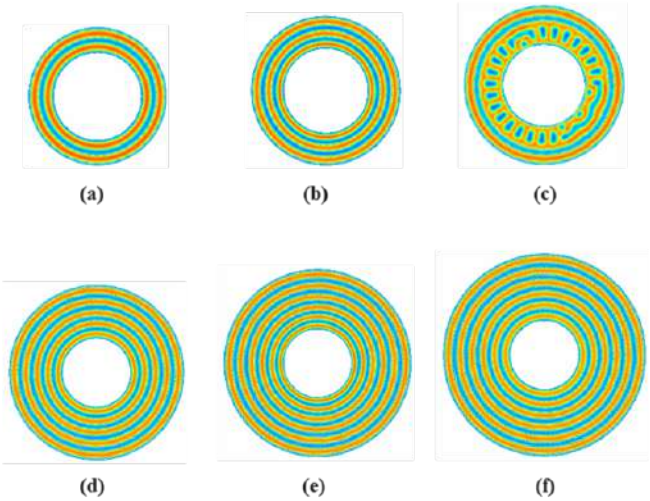

Figure 15. Asymmetric Lamellae forming system at r_a = 5 with neutral walls for various pore sizes d=3 in (a), d=4 in (b), d=5 in (c), d=8 in (d), d=9 in (e) and d=10 in (f).

Moreover, perforations started to show up in the morphologies contained in the biggest pores, indicating further relaxing due to a reduction in edge effects. Thus, morphology changed from highly oriented

concentric patterns subject to curvature at small sizes to more complex mixed structures coexisting with rings at larger diameters as well as the introduction of various strip alignments and eventual perforations as a result of increasingly relaxed boundaries.The asymmetric lamellae morphologies for polar geometries with attractive walls confined in circular annular pores are shown in Figure 15. The volume fractions of the blocks, f_a = 0.48 and f_b = 0.52, have been determined for the asymmetric study of diblock copolymers. To demonstrate the variation in pore diameters (d = 3, 4, 5, 8, 9, and 10), we fixed internal circles with radius r_a = 5 and external circles with radii r_b = 8, 9, 10, 13, 14, and 15. One million simulation runs were carried out. The interaction strength of the attractive walls was set at α = 0.2. Concentric circular lamellar structures emerged as the dominant morphology across most investigated pore sizes when the internal radius was increased from 3 to 5 units. This aligns with the significant influence of curvature effects on orientation enforcement.

However, the otherwise well-ordered morphology exhibited some deviations at the largest internal radius of 5 units. Among the concentric layers, some lamellar strips appeared parallel to the pore walls, and several perforated holes within the lamellar structure also exhibited distortion from their typical shapes. The fact that this disruption was limited to a pore radius of five units suggests that this size marked the point at which geometric constraints started to loosen enough to allow for the introduction of small abnormalities. Consequently, expanding the internal cavity mainly maintained concentric alignment up to 5 units, after which the quasi-cylindrical boundary allowed slightly disturbed concentric organization with a few parallel domains and distorted perforations, indicating a slight but noticeable loss of confinement oversight.

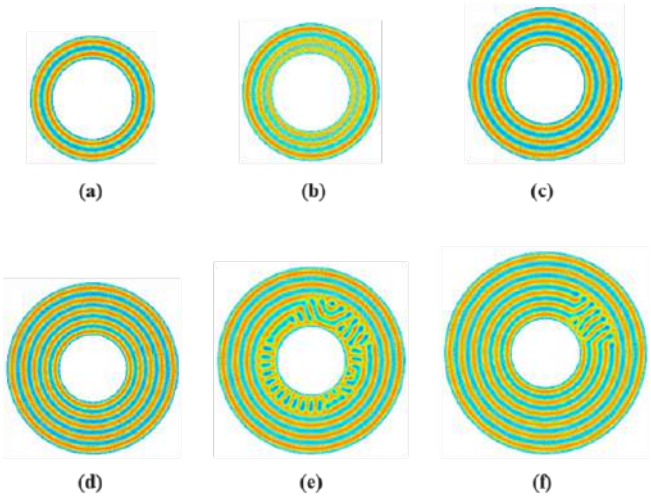

Figure 16. Asymmetric Lamellae forming system at r_a = 7 with neutral walls for various pore sizes d=3 in (a), d=4 in (b), d=5 in (c), d=8 in (d), d=9 in (e) and d=10 in (f).

Figure 16 displays the asymmetric lamellar morphologies for polar geometries with appealing walls. The block volume fractions for the asymmetric study of diblock copolymers, f_a = 0.48 and f_b = 0.52, have been determined. As an example, we fixed internal circles with radius r_a = 7 and external circles with radii r_b = 10, 11, 12, 15, 16, and 17 to demonstrate the difference in pore sizes for d = 3, 4, 5, 8, 9, and 10, respectively. There are one million simulation runs. Attractive walls have an interaction strength of α = 0.2. Strong curvature effects maintained the morphology tightly oriented in a circular pattern within the

lower pore diameters of 3, 4, and 5, while concentric circular lamellar structures formed when the internal pore radius increased from 5 to 7 units. Again, indicating curvature dominance, only concentric lamellae were seen at a slightly higher pore diameter of 8. But as the pore size increased to 9 and 10, deviations from the purely concentric morphology appeared. Size 9 showed partially concentric formations alongside newly developed perforated holes, signaling the beginning of relaxation from confinement, while size 10 additionally included clustered strips oriented perpendicular to the pore wall.

Thus, there was a transition from concentric-only patterns at smaller pore sizes to curved orientation with asymmetric features like holes and non-concentric domains at higher diameters, as the enlarging boundaries began to release more control over self-assembly beyond pore size 8.

3.6 Comparison with experimental study

Unlike experiments, computational modelling uses simulation techniques to study lamellae formation and determine the effects of pore shape, composition, and wall interactions. An understanding of directed self-organization is provided by both theoretical and empirical methods, which when combined, strengthen the analysis of block copolymer phase behaviour under confinement. Empirical validation of computer models is achieved through experimental research, which visualizes constructed morphologies under various real-world settings [6, 18, 30, 32, 43, 44].

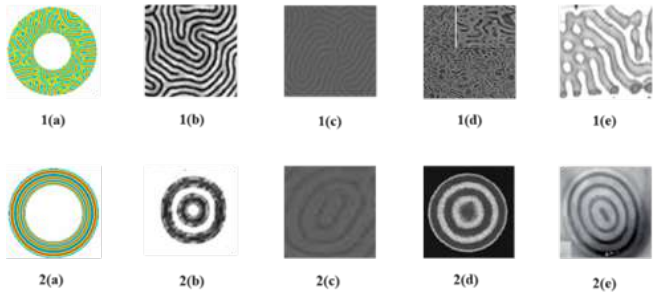

Figure 17. Comparison of predicted morphologies 1(a) and 2(a) with experimental studies, 1(b) Directing block copolymer self-assembly on patterned substrates, 1(c) and 2(c) Study of the ordered assembly morphologies of diblock copolymers on the same substrate, 1(d) Thin film morphologies of bulk-gyroid polystyrene-block polydimethylsiloxane under solvent vapour annealing, 1(e) Nanoscale patterning with block copolymers, 2(b) Morphology of symmetric block copolymer in a cylindrical pore, 2(d) Directing the self-assembly of block copolymers, 2 (e) Self-assembly of diblock copolymers under confinement.

In Figure 17, Diblock copolymer lamellar morphology (1*a*) with neutral walls is anticipated by computational modelling using cell dynamics simulations. This morphology closely resembles experimental pore architectures 1(*b* – *e*) with higher curvature effects. Assembled nanopatterns from theoretical prediction and actual observation agree strongly when compared directly. Computational predictions of concentric circular morphologies 2(*a*) with appealing walls closely matched actual dartboard designs 2(*b* – *e*). Under these confining conditions, a strong agreement was also established between theoretically built structures and experimental results.

4 Conclusion

Polymeric molecules known as diblock copolymers are made up of two chemically different blocks that are joined together. They form organized nanoscale domains by self-assembly. Geometric limitations imposed by containing diblock copolymers inside precisely sized nanopores can affect the shape of the copolymer self-assembly process. Cell dynamics simulations facilitate the modeling of self-assembly behavior in confinement and the observation of ensuing molecular morphologies. There are several levels of confinement, ranging from weak to strong, depending on the pore diameter. This affects the restricted copolymers' chosen morphology. Another parameter that is varied in the simulations is the surface contact strength between the copolymer blocks and the pore interface. Increased surface affinity often causes one block of wetness at the interface, which has an impact on interior self-assembly. The goal of the effort was to map out and predict in a systematic way the many morphologies that arise under certain combinations of surface energy and confinement strengths. This provides information about creating nanostructures with diblock copolymer self-assembly inside different sized patterned nanopores. When diblock copolymers are trapped in circular nanopores, lamellar structures alternating layers of the two block domains are seen experimentally. In certain circumstances, the restricted diblock copolymers also self-assemble into lamellar structures in the cell dynamics simulations carried out for this work. The simulations' predictions of lamellar patterns agree well with the results of the experiments. This proves that the behavior of diblock copolymers during self-organization and self-assembly at the nanoscale under confinement can be precisely simulated and predicted using cell dynamics models. In particular, the diblock copolymers arrange themselves as either parallel-to-the-curvature circular lamellae or concentric circular lamellae. This happens to pore walls that attract one block domain and to neutral pore walls that have no preferential attraction for either block. The finding confirms that computer modeling is a dependable method for understanding the mechanics and reproducing self-assembly processes at the nanoscale length scale. The diblock copolymer's self-assembly is significantly guided by the curvature of the circular nanopores. Parallel to the curvature, they arrange themselves into alternating lamellar or concentric circular patterns. The organization is also affected by the surface energy or affinity between the pore interface and the copolymer blocks. Positive user interfaces produce unique "dartboard patterns". The work provides fresh perspectives on the effects of confinement and interfacial interactions on diblock copolymer self-assembly by adjusting the curvature and surface energy parameters. Most importantly, there is a strong correlation between the nanostructures seen in experiments and models. This illustrates how useful computational modeling can be for logically and rationally creating novel materials before doing experiments. Self-assembling structures can be predicted by simulations, and parameters can be optimized for desired morphologies. This work creates a connection between simulation-generated controlled virtual worlds and industrial outcomes that can be achieved experimentally. Through the examination of block copolymer self-assembly inside precisely defined constrained geometries, a more profound comprehension of self-organization mechanisms is gained. The acquired knowledge has implications for guided self-assembly of block copolymers to create complex nanostructured materials. Due to the ability to arrange block copolymers into ordered structures, biomaterials and nanotechnological devices are among the potential uses. Future research will examine additional system features like various polymer topologies and pore geometries. This will contribute to the expansion of the found structure-property connections and offer more design recommendations for the synthesis of materials.

Author Contributions

Muhammad Javed Iqbal: Conceptualization, Methodology, Simulation. **Inayatullah Soomro**: Supervision, validation. **Maryam Bibi**: Reviewing and Editing. **Rab Nawaz Mallah**: Software.

Compliance with Ethical Standards

No conflict of interest among the authors.

Funding Information

Self

Author Information

ORCID:
Muhammad Javed Iqbal: 0009-0000-1737-1826
Inayatullah Somroo: 0000-0001-6423-1009

References

[1] Bae, S., Noack, M. M. and Yager, K. G. [2023], 'Surface enrichment dictates block copolymer orientation', *Nanoscale* **15**(15), 6901–6912.

[2] Beardsley, T. and Matsen, M. [2021], 'Fluctuation correction for the order–disorder transition of diblock copolymer melts', *The Journal of Chemical Physics* **154**(12).

[3] Cai, D., Li, J., Ma, Z., Gan, Z., Shao, Y., Xing, Q., Tan, R. and Dong, X.-H. [2022], 'Effect of molecular architecture and symmetry on self-assembly: A quantitative revisit using discrete aba triblock copolymers', *ACS Macro Letters* **11**(4), 555–561.

[4] Chen, P., Liang, H. and Shi, A.-C. [2008], 'Microstructures of a cylinder-forming diblock copolymer under spherical confinement', *Macromolecules* **41**(22), 8938–8943.

[5] Cheng, C.-H., Masuda, S., Nozaki, S., Nagano, C., Hirai, T., Kojio, K. and Takahara, A. [2020], 'Fabrication and deformation of mechanochromic nanocomposite elastomers based on rubbery and glassy block copolymer-grafted silica nanoparticles', *Macromolecules* **53**(11), 4541–4551.

[6] Darling, S. [2007], 'Directing the self-assembly of block copolymers', *Progress in polymer science* **32**(10), 1152–1204.

[7] Deepthi, K., Stamm, M. and Gowd, E. B. [2020], 'Factors influencing the formation of block copolymer-based supramolecular assemblies in bulk and thin films', *Materials Today Communications* **24**, 101147.

[8] Deng, Z. and Liu, S. [2020], 'Emerging trends in solution self-assembly of block copolymers', *Polymer* **207**, 122914.

[9] Diaz, J., Pinna, M., Breen, C., Zvelindovsky, A. and Pagonabarraga, I. [2023], 'Block copolymer nanocomposites under confinement: Effect on frustrated phases', *Macromolecules* **56**(13), 5010–5021.

[10] Diaz, J., Pinna, M., Zvelindovsky, A. V. and Pagonabarraga, I. [2019], 'Large scale three dimensional simulations of hybrid block copolymer/nanoparticle systems', *Soft matter* **15**(45), 9325–9335.

[11] Doi, M. [2013], *Soft matter physics*, Oxford University Press, USA.

[12] Garcia, R. [2020], 'Nanomechanical mapping of soft materials with the atomic force microscope: methods, theory and applications', *Chemical Society Reviews* **49**(16), 5850–5884.

[13] Goswami, M., Iyiola, O. O., Lu, W., Hong, K., Zolnierczuk, P., Stingaciu, L.-R., Heller, W. T., Taleb, O., Sumpter, B. G. and Hallinan Jr, D. T. [2023], 'Understanding interfacial block copolymer structure and dynamics', *Macromolecules* **56**(3), 762–771.

[14] Gupta, S. and Chokshi, P. [2020], 'Confinement-induced ordering of grafted nanoparticles aided by diblock copolymers', *Journal of Applied Physics* **127**(7).

[15] Herschberg, T., Carrillo, J.-M. Y., Sumpter, B. G., Panagiotou, E. and Kumar, R. [2021], 'Topological effects near order–disorder transitions in symmetric diblock copolymer melts', *Macromolecules* **54**(16), 7492–7499.

[16] Karayianni, M. and Pispas, S. [2021], 'Block copolymer solution self-assembly: Recent advances, emerging trends, and applications', *Journal of Polymer Science* **59**(17), 1874–1898.

[17] Khaksar, E., Golshan, M., Roghani-Mamaqani, H. and Salami-Kalajahi, M. [2023], 'Confinement effect of blocks on morphology of composite particles in co-assembly of block copolymers/homopolymers', *Polyolefins Journal* .

[18] Krishnamoorthy, S., Hinderling, C. and Heinzelmann, H. [2006], 'Nanoscale patterning with block copolymers', *Materials Today* **9**(9), 40–47.

[19] Kumar, R., Kumar, M. and Luthra, G. [2023], 'Fundamental approaches and applications of nanotechnology: A mini review', *Materials Today: Proceedings* .

[20] LeVeque, R. J. [2007], *Finite difference methods for ordinary and partial differential equations: steady-state and time-dependent problems*, SIAM.

[21] Li, H., Mao, X., Wang, H., Geng, Z., Xiong, B., Zhang, L., Liu, S., Xu, J. and Zhu, J. [2020], 'Kinetically dependent self-assembly of chiral block copolymers under 3d confinement', *Macromolecules* **53**(11), 4214–4223.

[22] Li, Z. and Lin, Z. [2022], 'Self-assembly of block copolymers for biological applications', *Polymer International* **71**(4), 366–370.

[23] Lodge, T. P., Seitzinger, C. L., Seeger, S. C., Yang, S., Gupta, S. and Dorfman, K. D. [2022], 'Dynamics and equilibration mechanisms in block copolymer particles', *ACS polymers Au* **2**(6), 397–416.

[24] Malik, S., Muhammad, K. and Waheed, Y. [2023], 'Nanotechnology: A revolution in modern industry', *Molecules* **28**(2), 661.

[25] Murat, M., Grest, G. S. and Kremer, K. [1999], 'Statics and dynamics of symmetric diblock copolymers: A molecular dynamics study', *Macromolecules* **32**(3), 595–609.

[26] Pinna, M. and Zvelindovsky, A. [2012], 'Large scale simulation of block copolymers with cell dynamics', *The European Physical Journal B* **85**, 1–18.

[27] Ree, B. J., Satoh, Y., Isono, T. and Satoh, T. [2021], 'Influence of topological confinement on nanoscale film morphologies of tricyclic block copolymers', *Macromolecules* **54**(9), 4120–4127.

[28] Rongqiao, Y., Baohui, L. and An-Chang, S. [2012], 'Phase behavior of binary blends of diblock copolymer/homopolymer confined in spherical nanopores'.

[29] Rosedale, J. H., Bates, F. S., Almdal, K., Mortensen, K. and Wignall, G. D. [1995], 'Order and disorder in symmetric diblock copolymer melts', *Macromolecules* **28**(5), 1429–1443.

[30] Sevink, G., Zvelindovsky, A., Fraaije, J. and Huinink, H. [2001], 'Morphology of symmetric block copolymer in a cylindrical pore', *The Journal of Chemical Physics* **115**(17), 8226–8230.

[31] Sevink, G. and Zvelindovsky, A. V. [2008], 'Block copolymers confined in a nanopore: Pathfinding in a curving and frustrating flatland', *The Journal of chemical physics* **128**(8).

[32] Shi, A.-C. and Li, B. [2013], 'Self-assembly of diblock copolymers under confinement', *Soft Matter* **9**(5), 1398–1413.

[33] Song, S., Zhou, H., Manners, I. and Winnik, M. A. [2021], 'Block copolymer self-assembly: Polydisperse corona-forming blocks leading to uniform morphologies', *Chem* **7**(10), 2800–2821.

[34] Stewart-Sloan, C. R. and Thomas, E. L. [2011], 'Interplay of symmetries of block polymers and confining geometries', *European polymer journal* **47**(4), 630–646.

[35] Sun, Y., Tan, R., Ma, Z., Gan, Z., Li, G., Zhou, D., Shao, Y., Zhang, W.-B., Zhang, R. and Dong, X.-H. [2020], 'Discrete block copolymers with diverse architectures: resolving complex spherical phases with one monomer resolution', *ACS central science* **6**(8), 1386–1393.

[36] Wang, Z., Chan, C. L. C., Zhao, T. H., Parker, R. M. and Vignolini, S. [2021], 'Recent advances in block copolymer self-assembly for the fabrication of photonic films and pigments', *Advanced Optical Materials* **9**(21), 2100519.

[37] Wong, C. K., Qiang, X., Müller, A. H. and Gröschel, A. H. [2020], 'Self-assembly of block copolymers into internally ordered microparticles', *Progress in Polymer Science* **102**, 101211.

[38] Wu, J., Chen, S.-T., Li, S.-B., Liu, L.-M., Wang, X.-H. and Lang, W.-C. [2023], 'Simulation of surface-induced morphology transition and phase diagram of linear triblock copolymers under spherical confinement', *Chinese Journal of Polymer Science* **41**(1), 166–178.

[39] Wu, Y., Cheng, G., Katsov, K., Sides, S. W., Wang, J., Tang, J., Fredrickson, G. H., Moskovits, M. and Stucky, G. D. [2004], 'Composite mesostructures by nano-confinement', *Nature materials* **3**(11), 816–822.

[40] Xiang, L., Li, Q., Li, C., Yang, Q., Xu, F. and Mai, Y. [2023], 'Block copolymer self-assembly directed synthesis of porous materials with ordered bicontinuous structures and their potential applications', *Advanced Materials* **35**(5), 2207684.

[41] Xiao, X., Huang, Y., Liu, H. and Hu, Y. [2007], 'Morphology transition of block copolymers under curved confinement', *Macromolecular theory and simulations* **16**(8), 732–741.

[42] Yang, J., Dong, Q., Peng, L., Huang, X. and Li, W. [2023], 'Transition paths of ordered phases in a diblock copolymer under cylindrical confinement', *Macromolecules* .

[43] Yu, C. and Xiong, S. [2020], 'Directed self-assembly of block copolymers for sub-10 nm fabrication [j]', *International Journal of Extreme Manufacturing* **2**(03), 129–162.

[44] Zhang, B., Meng, L. and Li, Z. [2022], 'Study of the ordered assembly morphologies of diblock copolymers on the same substrate', *RSC advances* **12**(44), 28376–28387.

[45] Zhang, H., Clothier, G. K., Guimarães, T. R., Kita, R., Zetterlund, P. B. and Okamura, Y. [2022], 'Tuning phase separation morphology in blend thin films using well-defined linear (multi) block copolymers', *Polymer* **240**, 124466.

[46] Zhao, X., Chen, X., Yuk, H., Lin, S., Liu, X. and Parada, G. [2021], 'Soft materials by design: unconventional polymer networks give extreme properties', *Chemical Reviews* **121**(8), 4309–4372.